JOURNAL OF CATALYSIS 40, 226–235 (1975)

A Nuclear Magnetic Resonance Investigation of High Surface Area Silica–Aluminas

L. B. SCHREIBER AND R. W. VAUGHAN

Division of Chemistry and Chemical Engineering, California Institute of Technology, Pasadena, California 91125

Received April 16, 1975

A combination of conventional and multiple pulse nuclear magnetic resonance (NMR) techniques has been used to examine the hydroxyl protons on a series of high surface area silica–aluminas whose composition varied from 0–100% SiO_2. Protons remaining on these materials after being calcined at 500°C are found to exist as immobile and widely separated hydroxyl groups at room temperature. The concentrations of both SiOH and AlOH groups are reported as a function of adsorbent composition. With the high silica content samples, 100–75% SiO_2, no AlOH groups were detectable, while on the 50% and lower SiO_2 content samples most surface protons were in AlOH groups; thus, there is indication of a major change in local structure between 75 and 50% silica content. The isotropic part of the chemical shift tensor for hydroxyls on pure SiO_2 is −4.2 ppm relative to TMS and the anisotropy extracted from the powder pattern assuming an axially symmetric tensor is +6.9 ppm, substantially smaller than those found for hydroxyl groups in the solid state.

INTRODUCTION

This paper presents results of a nuclear magnetic resonance (NMR) study of hydroxyl protons bound to the surface of silica–aluminas whose composition varied from 0 to 100% SiO_2. The surface hydroxyl groups on high surface area silica have been extensively studied, particularly by infrared (*1,2*) and NMR techniques (*3–8*). Some NMR studies have been reported of hydroxyl groups on an 87.5% silica–12.5% alumina sample (*5,9,10*) and on pure alumina (*11,12*). However, the present work represents to the authors' knowledge the only attempt using NMR to examine surface hydroxyls on a whole series of silica–aluminas. In addition, a variety of "multiple pulse" NMR techniques have been used in this work in addition to conventional pulsed NMR, and thus some of the difficulties associated with the interpretation of NMR results for surface species have been avoided.

EXPERIMENTAL DETAILS

Sample preparation. The samples used in this work were prepared by Dr. D. A. Hickson at the Chevron Laboratories in Richmond, Calif., and have been the subject of a publication by Schwarz (*13*) where selective adsorption coupled with infrared techniques was used to characterize the nature of the acid sites on the surfaces. The samples were prepared by mixing desired amounts of $AlCl_3$ and tetraethyl ortho silicate in methanolic solution (*14*). The resulting solution was homogeneously gelled by the addition of propylene oxide, thus raising the pH. The methanol was then displaced by rinsing in diethyl ether. The material was then placed in an autoclave, and the temperature was brought to the critical point for diethyl ether. The vapor was flushed away with dry nitrogen. This resulted in an extremely high surface area material. Infrared techniques were used to demonstrate that hydroxyl groups in these mate-

rials rapidly exchanged with D_2O vapor and thus represent surface groups (*15*).

Sample pretreatment. A cavity for containment of each sample was formed from a 15-cm length of 4-mm quartz tubing by blowing out the bottom 10 mm of the tube to 5 mm o.d. and then sealing that end. This procedure produced a cavity with an i.d. of 4.5 mm which was packed with the sample, containing typically 20–40 mg of material with a surface area of 12 to 24 m^2. The open end of each tube was attached to a glass vacuum system of 2-liter volume for treatment of the samples. The vacuum system was greaseless and produced a pressure of 10^{-7} Torr. Two samples of each composition were prepared. The first sample was calcined in 152 Torr of oxygen for 1 hr at 500°C and then sealed. The second sample, after being calcined for 1 hr at 500°C, was cooled to 150°C and exposed to water vapor at 4.6 Torr for 1 hr, evacuated, and then sealed.

NMR apparatus. The NMR measurements were conducted at room temperature and at 56.4 MHz. Signal averaging was used (256 decays) and an external deuterium lock system held the magnet field drift to a few milligauss during the period of several hours normally needed for signal averaging (T_1's were all in the 20-sec range). Free induction decay spectra were taken well off resonance (50 kHz) and the envelope of the observed oscillation used to determine the decay. This technique involves giving up a substantial portion of the available signal to noise and accounts for much of the experimental scatter observed in Figs. 1–5. However, it assures that the reported decays are not contaminated by artifacts.

The basic multiple pulse NMR spectrometer has been previously described (*16*). The sample coil was constructed as earlier reported to minimize rf inhomogeneity (*17*), and the quality factor, Q, of the probe was 40. It was found necessary to use components constructed with Teflon dielectric for items in and near the probe to eliminate anomalous proton signals.

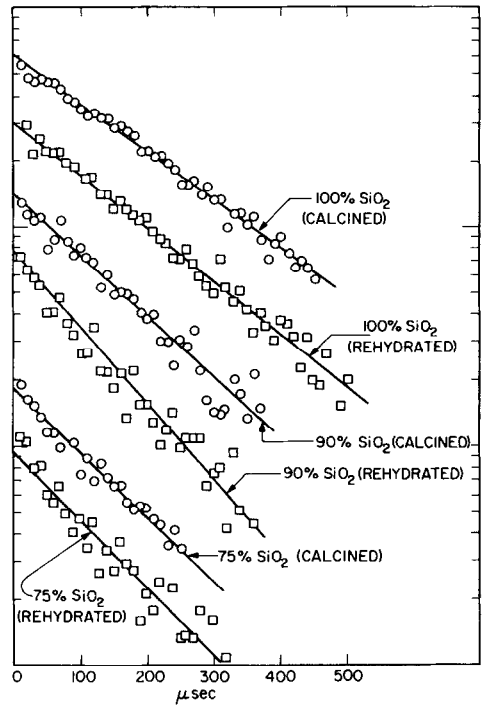

FIG. 1. Plot of free induction decay envelope vs time for samples of varying SiO_2 composition. Data from the various samples have been displaced vertically in order to clarify presentation. The values of T_2 reported in Table 1 were obtained from the slopes of the lines placed through the data.

The presence of any small transients due to pulse overload of the receiving circuits can mask the low-level signals available from these measurements. Thus, several pulse buffers were installed which improved the receiver overload characteristics. Each pulse buffer was a passive circuit consisting of a Relcom BT9 transformer (*18*) to increase impedence of the signal to 800 ohms, three sets of crossed diodes (germanium IN270) across the 800 ohms (for clipping the rf pulse), and a second Relcom BT9 to transform the signal back to 50 ohms. Such buffers limited pulses of several volts at the input to ~70 mV rms at the output with an attenuation of the low-level signals of 6 dB. In addition to using such a buffer before the receiver,

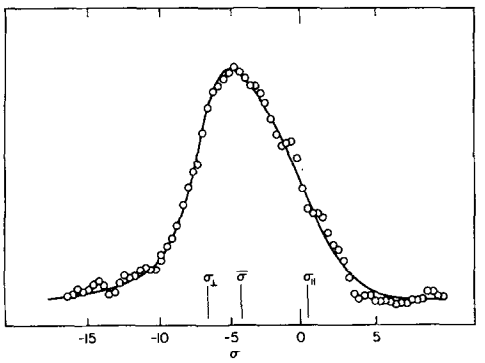

FIG. 2. Powder pattern using eight-pulse cycle of 100% SiO_2 calcined sample. The signal amplitude is plotted vs chemical shift (ppm) relative to TMS.

it was found advantageous to place a buffer between several of the Avantek unit amplifiers (*19*) used in the receiver. Apparently this allowed one to minimize the poorly understood nonlinear overload characteristics of these particular unit amplifiers. Under these conditions the small signals from these experiments could be characterized approximately 4 μ after the end of the rf pulse.

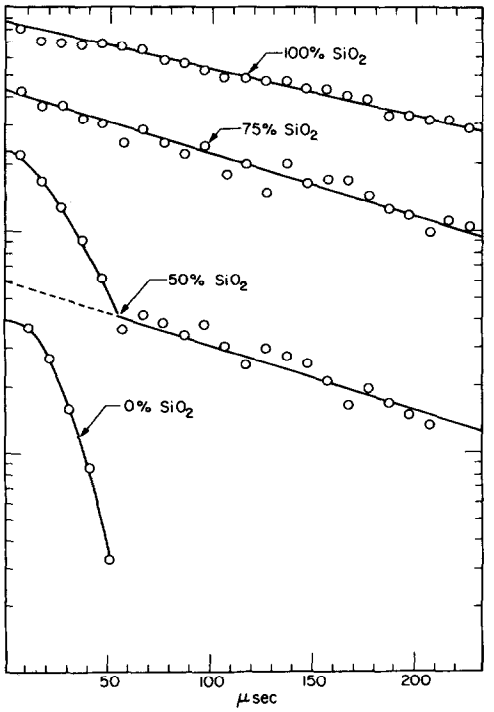

FIG. 3. Plot of free induction decay envelope vs time for calcined samples of varying SiO_2 composition. Data from the various samples have been displaced vertically in order to clarify presentation.

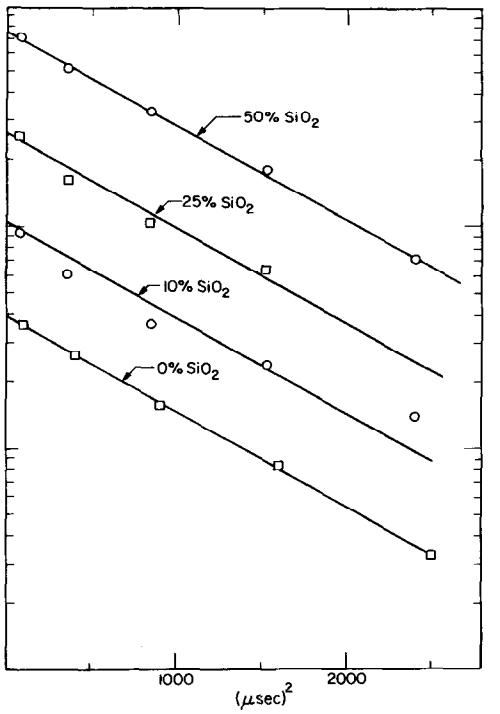

FIG. 4. Plot of decay envelope of AlOH groups vs time squared for calcined samples of varying SiO_2 composition. Data from the various samples have been displaced vertically in order to clarify presentation. The values of second moment reported in Table 1 were obtained from the slopes of the lines placed through the data.

The data acquisition system consisted of a Biomation 802 transient recorder interfaced to a PDP8/e computer equipped with a PDP TU60 tape cassette data storage system.

NMR techniques. The application of NMR techniques has furnished information on the (a) number, (b) arrangement, (c) bonding, and (d) motion of hydroxyl groups on the materials studied.

(a) The number, or density, of hydroxyls on the materials was determined from the initial magnitude of the free induction decay observed after a 90° pulse. Care has

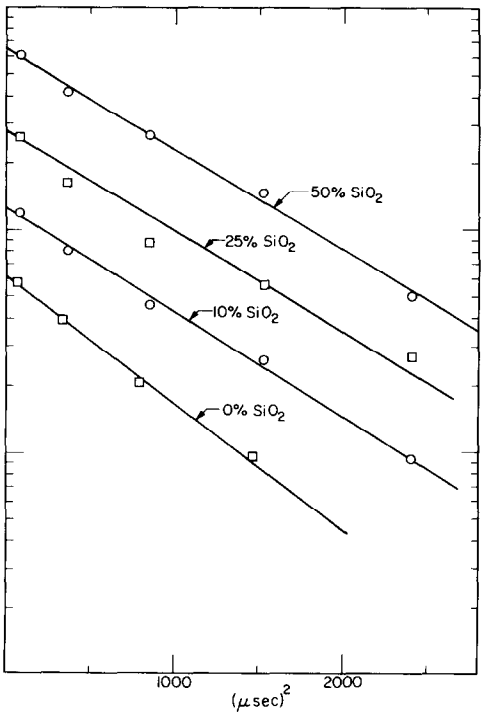

FIG. 5. Plot of decay envelope of AlOH groups vs time squared for rehydrated samples of varying SiO_2 composition. Data from the various samples have been displaced vertically in order to clarify presentation. The values of second moment reported in Table 1 were obtained from the slopes of the lines placed through the data.

to be taken that the sample is at equilibrium with the magnetic field before application of the 90° pulse. The magnitude of the free induction decay was calibrated by using samples of known proton content.

(b) Information on the local environment and arrangement of hydroxyl groups on the surface was obtained from an analysis of the free induction decay lineshape, either directly or by use of a moment analysis (*20*).

(c) Information on the chemical bonding of the hydroxyl groups to these materials has been obtained by using the multiple pulse NMR techniques (*21*) to measure components of the chemical shift tensor. The chemical shift tensor results from a coupling of the electronic wavefunctions with the nuclei and, thus, mirrors changes in electronic structure brought about by chemical bonding.

(d) Motion of the protons can alter, or average, both the dipolar interactions responsible for the free induction decay lineshape and the chemical shift tensor and, in addition, can control the magnitude of a variety of relaxation times. The effect of motion on a variety of NMR relaxation times has been extensively reviewed with special emphasis on surface systems (*3–8*).

The use of conventional pulsed NMR techniques has been extensively discussed (*22*), and the comments here are limited to a discussion of the multiple pulse techniques and a discussion of the chemical shift tensor.

Multiple pulse NMR techniques. As the above discussion indicates, several interactions contribute simultaneously to both the lineshape and associated relaxation effects of an NMR resonance. Although each of these interactions contains useful information, usually the NMR spectrum can be interpreted to give only the largest one or some complex combination of several. To allow further separation and characterization of the interactions present, a variety of recently developed multiple pulse NMR techniques may be used. These are, in general, characterized by the application of periodic and cyclic chains of intense rf pulses and have the effect of altering the effective size and character of specific interactions. Thus, use of these techniques can allow measurement of small interactions which are normally not measureable due to the presence of much larger interactions and can allow separation of interactions normally only measurable as a sum. Three such sequences were used in this work and are described below.

An eight-pulse cycle was used to remove the effects of static homonuclear dipolar broadening and to allow measurement of the proton chemical shift tensor. This pulse sequence has been discussed in

detail previously (*17,23*), and it will only be pointed out here that it is essential to have the characteristic time associated with the pulse cycle shorter than the spin–spin relaxation time (the inverse of the dipolar linewidth), and that motional effects, particularly in the 10^{-4} to 10^{-6} sec time domain, can interfere with the averaging process.

A phase altered version of the eight-pulse cycle (*23,24*) was also used in this work. This sequence has the ability to remove the effect of static magnetic field inhomogeneities in addition to homonuclear dipolar interactions from the NMR spectrum. Thus, it can be used to determine what portion of the linewidth observed in the regular eight-pulse spectrum is due to magnetic field inhomogeneities. As the chemical shift is, in effect, a magnetic field inhomogeneity, the phase altered eight-pulse cycle furnishes a means to be sure that the linewidth observed in the eight-pulse cycle can be attributed to chemical shift anisotropy and not to motional effects, experimental problems, or any residual homonuclear dipolar effects.

A Carr–Purcell sequence has been used here to separate the total dipolar interaction into contributions from homonuclear and heteronuclear interactions. The Meiboom-Gill (*22*) modification was used with the slight modification that two closely spaced 90° pulses were used instead of a single 180° pulse. By using previously described pulse adjustment procedures (*16*), very precise 180° pulse rotations could be assured. The signal was sampled between each 180° rotation.

Chemical shift tensor. The electron distribution surrounding a nucleus can distort the magnetic field at the nuclear site, and consequently, one observes a dependence of the resonance frequency on the nature of the chemical bonding present. As the electronic environment is normally not isotropic, this frequency dependence will show an angular dependence and is described by a chemical shift tensor. For the high field case this is a symmetric tensor and normally described by the three principal values of the tensor and the orientation of the principal axis coordinate system. The frequency shift induced by the chemical shift is normally not measurable in solids, but by using the multiple pulse NMR techniques to remove the dipolar broadening, it can be accurately determined. In single crystal samples one can determine both the principal values and the orientation of the principal axis system. However, in polycrystalline powders like the ones studied in this paper, one has present simultaneously many different orientations so that one observes a spectrum broadened by chemical shift effects. This "powder pattern" can be analyzed to extract the magnitude of the three principal values (*25*).

RESULTS AND DISCUSSION

100% Silica. The semilogarithmic plot of the free induction decay for the calcined sample of pure silica is shown in Fig. 1. As shown, the decay is exponential within the precision of the data. By extrapolating the line in Fig. 1 back to zero time, an initial intensity is obtained which indicates 1.6 protons/100 Å^2 ± 10% and a ratio of silicon atoms to protons of 11. The hydroxyl concentrations for silica samples treated at 500°C were found in the range 1.6–2.3 protons/100 Å^2 by Davydov and coworkers (*26*), using chemical methods of analysis and a variety of preparation techniques. O'Reilly *et al.* (*9*) found 2.6 protons/100 Å^2, and more recently Freude *et al.* (*27*) measured 0.87 protons/100 Å^2, both using NMR techniques.

The time constant, T_2, for the free induction decay is 200 μsec, and as an exponential decay in time space is equivalent to a Lorentzian line in frequency space, this is equivalent to a Lorentzian absorption spectrum with a full width at half height of 1600 Hz. A Lorentzian lineshape

has been previously observed by O'Reilly and co-workers (*5,9*), who reported a T_2 of 180 μsec which did not vary as a function of temperature between −210 and 280°C. Both the lack of a temperature dependence and results of the multiple pulse NMR measurements discussed below indicate that the Lorentzian lineshape is not the result of motional averaging. Lorentzian lineshapes have been predicted for a number of geometries where it is assumed that spins are distributed in a random fashion over only a small fraction of possible sites (*28*). It does not appear possible to use the results of such analytic treatments to extract quantitative information on the distribution of hydroxyls on the silica. However, because the decay time is large, i.e., 200 μsec, it can be concluded that the protons are widely separated. Specifically, the proton–proton distances are greater than about 4 Å, which thus excludes the possibility of adsorbed water on the silica surface, but does not exclude having two hydroxyl groups attached to the same silicon [see Peri and Hensley (*29*)].

The eight-pulse cycle, with a cycle time of 96 μsec, was applied to the calcined sample. As shown in Fig. 2, the linewidth collapsed to near 250 Hz. One can conclude that the width and Lorentzian shape of the free induction decay were determined almost completely by dipolar interactions and furthermore that the dipolar interactions were essentially static on the timescale of 10^{-4} to 10–6 sec. This furnishes evidence for the interpretation given above of the free induction decay lineshape.

The lineshape produced by the multiple pulse experiment has several potential sources: (a) inhomogeneous broadening, primarily chemical shift coupling, (b) time dependence, particularly in the dipolar interaction, and (c) residual instrumental broadening. The phase altered eight-pulse cycle was applied to further separate these effects as it will remove inhomogeneous broadening as well as static dipolar broadening. The line collapsed further to 32 Hz under the influence of the phase altered eight-pulse sequence, thus indicating that the lineshape in Fig. 2 can be attributed to a chemical shift powder pattern broadened by bulk susceptibility effects. The smooth line through the data points in Fig. 2 is a computer fit for an axially symmetric chemical shift tensor with a Lorentzian broadening function. The principal values furnished by the fit are $\sigma_\perp = -5.1$ ppm and $\sigma_{/\!/} = +1.8$ ppm relative to a spherical sample of tetramethylsilane (±1 ppm). In order to correct values for the effects of bulk susceptibility, the sample was approximated by an ellipsoid ($a = b = 0.5\ c$, where a, b, and c are the semiaxes and with the magnetic field being along a), and the tabulated values of Osborn (*30*) were used with a value of -1.13×10^{-6} for the volume susceptibility to calculate a susceptibility correction of −1.4 ppm. Thus, susceptibility independent principal values for the hydroxyl protons on silica are $\sigma_\perp = -6.5$ ppm and $\sigma_{/\!/} = +0.4$ ppm, and a susceptibility independent value for the trace, or isotropic portion, is −4.2 ppm (relative to TMS). A Lorentzian broadening function with a width of near 6 ppm was required to fit the spectrum in Fig. 2, and this width is attributed primarily to smearing of the magnetic field at the surface of a particle whose magnetic susceptibility is different from the medium it is in.

A number of studies have recently been reported of the chemical shift tensor of both hydrogen bonded (*31*) and nonhydrogen bonded (*32*) hydroxyl protons, and all have reported tensors which exhibit an anisotropy ($\sigma_{/\!/} - \sigma_\perp$) from 2 to 4 times the size of the 6.9 ppm found in this study. One can conclude either that the surface hydroxyl groups studied here have substantially altered chemical bonding from these solid state systems or that the value measured here has been partially averaged by an angular motion of the O—H vector

(i.e., a wagging or rotation of the hydroxyl bond around the oxygen). Thus, while NMR data indicate that major motion, diffusion from oxygen site to oxygen site, does not occur, there is some indication that a local reorientation of the hydrogen around its oxygen may occur in this system. Hopefully, this point can be clarified by performing the multiple pulse measurements at low temperatures.

The same series of NMR measurements has been made on the rehydrated sample of 100% silica with almost identical results. A surface concentration of 1.9 protons/100 Å^2 was determined from the free induction decay. This small increase of 0.3 protons/100 Å^2 suggests that the rehydration by water vapor is not reversible. Such irreversible rehydration has been reported earlier for silicas heat treated at temperatures over 400°C both by Young (*33*) and by Hockey and Pethica (*34*).

The lineshape for the rehydrated sample was Lorentzian within the precision of the data and indicates that the water molecules which were absorbed went on the surface as widely separated hydroxyl groups. The principal values for the chemical shift tensor were determined as above and found to be $\sigma_\perp = -6.2$ ppm and $\sigma_{//} = +0.6$ ppm, which are identical within experimental accuracy with the nonhydrated sample. Thus, essentially no difference between the two samples could be determined except for the small concentration difference noted above.

0% Silica (100% alumina). The logarithm of the amplitude of the free induction decay for the calcined alumina sample is shown versus time in Fig. 3 and versus time squared in Fig. 4. The proton concentration was 3.1 protons/100 Å^2, and the ratio of aluminum atoms to protons was 6.7. This higher concentration of protons on alumina compared to silica has been pointed out before (*35*). The linear plot in Fig. 4 is the time response expected of a decay associated with a Gaussian lineshape, and from the slope of the line through the data points, one estimates a second moment of 2.8 G^2 for the proton line. This second moment has contributions from proton–proton interactions (homonuclear) and from proton–aluminum interactions (heteronuclear), and in order to separate these, a Car–Purcell–Meiboom–Gill cycle was applied with a pulse spacing of 50 μsec. Assuming a Gaussian lineshape for the envelope of the echo maxima, an estimate of near 0.2 G^2 was obtained for the second moment. As the Carr–Purcell–Meiboom–Gill sequence removes static heteronuclear dipolar broadening as well as magnetic field inhomogeneity effects, the 0.2 G^2 can be attributed to homonuclear dipolar broadening (i.e., proton–proton broadening). This would imply that 2.6 G^2 of the proton second moment (i.e., essentially all of the 2.8 G^2 second moment measured) can be attributed to the heteronuclear (proton–aluminum) dipolar interaction. Also note that the small size of the proton–proton second moment implies widely separated protons on the alumina surface.

The rehydrated sample of alumina has a still higher concentration of hydroxyl groups, 4.4/100 Å^2, and was Gaussian within the experimental error, as indicated in Fig. 5. The second moment estimated from the slope of the line through the data points in Fig. 5 is 3.7 G^2.

Silica–aluminas. Compositions of 10, 25, 50, 75, and 90% silica were prepared, treated, and investigated as described above for the pure SiO_2 and Al_2O_3. Experimental results are presented in Figs. 1, 3, 4, and 5 and in Table 1. A number of conclusions can be drawn from these results.

The 90 and 75% SiO_2 samples exhibited a single exponential decay for both calcined and rehydrated samples as shown in Fig. 1. The concentrations of protons on these samples and estimates of the decay

TABLE 1
SUMMARY OF PROTON NMR RESULTS FOR CALCINED AND REHYDRATED SILICA–ALUMINAS OF VARYING COMPOSITION

		Calcined samples				Rehydrated samples			
		SiOH		AlOH		SiOH		AlOH	
SiO_2 (wt %)	Surface area (m^2/g)	No. H/100 Å^2	T_2 (μsec)	No. H/100 Å^2	M_2 (G^2)	No. H/100 Å^2	T_2 (μsec)	No. H/100 Å^2	M_2 (G^2)
100	576	1.6	200	—	—	1.9	170	—	—
90	693	1.5	160	—	—	3.2	120	—	—
75	615	1.2	150	—	—	1.8	140	—	—
50	727	1.0	140	2.7	2.7	1.0	105	3.5	2.9
25	839	0.2	160	2.4	2.7	0.5	80	3.7	2.9
10	768	—	—	3.4	2.7	—	—	4.4	3.0
0	571	—	—	3.1	2.8	—	—	4.4	3.7

constants are given in Table 1. Using results and arguments from the discussion of the pure silica sample, the measured decay constants indicate that protons on these samples do not exist as closely spaced pairs (i.e., not as absorbed water) and do not exist in close proximity to an aluminum ion (i.e., not as AlOH groups). Again one notes that exponential decays, or Lorentzian lineshapes have been predicted for a number of geometries where it is assumed spins are distributed in a random fashion over only a small fraction of possible sites (*28*). As in the case of pure silica, the eight-pulse sequence was applied to both the calcined and rehydrated 90% silica samples with results similar to those reported above for the pure silica, confirming that the observed decays were produced by static dipolar interactions.

The 50, 25, and 10% SiO_2 samples are quite different from the 75 and 90% samples. Figure 3 illustrates this point for the 50% SiO_2 calcined sample where a logarithmic plot is shown for the 100, 75, 50, and 0% calcined samples. The 50% SiO_2 decay consists of two components. At long times (>70 μsec) it is qualitatively and quantitatively similar to the 75 and 100% SiO_2 decays, while at short times it is similar to the 0% (pure alumina) decay. In the analysis of the data of the pure alumina, the short decay was found to be due to the aluminum–proton dipolar interaction and was associated with hydroxyl groups attached to aluminum ions, while in the analysis of the 100, 90, and 75% SiO_2, the long decays were associated with isolated hydroxyls attached to silicon ions, i.e., SiOH groups. It is thus possible to separate quantitatively the fraction of protons bound to silicon and that fraction bound to aluminum. The intercept of the extrapolated line which fits the long-time behavior, as shown in Fig. 3, is a measure of the SiOH density. The difference between this extrapolated intercept and the total intercept is a measure of the AlOH density on the sample. In order to compute this difference accurately, the 50% SiO_2 curve in Fig. 4 was constructed by subtracting the amplitudes of the line extrapolated from the long-time portion shown in Fig. 3 from the amplitudes of the data points in the short-time region. Thus, the 50% SiO_2 curve shown in Fig. 4 represents the signal from the AlOH groups, and the intercept is directly proportional to the concentration of hydroxyl groups bound to aluminum ions.

The decays observed for the 50% SiO_2 rehydrated sample and both of the 25% SiO_2 samples also consisted of two components. Like the 50% SiO_2 calcined sample, the long-time portion was similar to the 100% SiO_2 decay, and the short-time portion was similar to the 100% Al_2O_3 decay. The number of hydroxyl groups bound to silicon ions and the number to aluminum ions were calculated in the same manner as above for the 50% SiO_2 calcined sample. For both 10% SiO_2 samples, the decays were similar to the 0% SiO_2 samples.

In order to compute second moments for the AlOH groups, a Gaussian decay was assumed. As can be seen from Figs. 4 and 5, the straight lines, which are indicative of Gaussian behavior, fit the data for the 0 and 50% SiO_2 samples excellently, but fit the data for the 10 and 25% SiO_2 samples only moderately well. From the slopes of these lines, second moments were computed and are presented in Table 1. Almost all of the second moments for the AlOH groups were close to 2.8 G^2.

The entire results for the surface concentrations of AlOH groups and SiOH groups are presented in Table 1. It appears to be of substantial significance that AlOH groups were not detected on the 75% silica sample while nearly 75% of the protons on the 50% silica sample appear to be AlOH groups. Previous infrared work by Basila (*36*) has concluded that the existence of a single hydroxyl stretching frequency on a 75% silica implied only SiOH groups. Prior NMR work by O'Reilly *et al.* (*9*) and Hall *et al.* (*10*) on a 89% SiO_2 sample had limited the percentage of surface protons in AlOH groups to less than 20%. The 75% silica sample contains 1 aluminum ion for every 2.5 silicon ions, but no measurable AlOH groups; the 50% silica contains 1 aluminum ion for each 0.85 silicon ion (54% aluminum ions), yet 75% of the hydroxyls are bound to the aluminum. These samples are all amorphous in the sense that no X-ray spectra are obtainable and infrared data on Al–O and Si–O are broadened, yet the results presented here imply substantial order, specifically in the attachment of the hydroxyls.

There appears to be a clear qualitative change occurring in the nature of the hydroxyl groups between the 75 and 50% silica samples, with the 100, 90 and 75% being similar and exhibiting no detectable AlOH groups while the 50, 25, 10 and 0% SiO_2 have the bulk of their protons attached in close proximity to an aluminum ion. Further work on these samples involving infrared studies, surface titrations, and catalytic studies is in progress, and relationships between the NMR results and these studies will be published in the near future.

ACKNOWLEDGMENT

The aid and advice of James A. Schwarz were greatly appreciated. Assistance and discussions on receiver electronics with Michael E. Stoll are acknowledged. L. B. S. gratefully acknowledges support from a Union Oil Co. Fellowship and a National Science Foundation Energy-Related Traineeship. Support from National Science Foundation Grant No. 32517 is acknowledged as is support received from the Alfred P. Sloan Foundation and the Camille and Henry Dreyfus Foundation.

REFERENCES

1. Hair, M. L., "Infrared Spectroscopy in Surface Chemistry." Dekker, New York, 1967.
2. Little, L. H., "Infrared Spectroscopy of Adsorbed Species." Academic Press, New York, 1966.
3. Aston, J. G., *in* "The Solid-Gas Interface" (E. A. Flood, Ed.), Vol. 2, p. 895. Dekker, New York, 1967.
4. Derouane, E. G., Fraissard, J., Fripiat, J. J., and Stone, W. E. E., *Catal. Rev.* **7**, 121 (1972).
5. O'Reilly, D. E., *in* "Advances in Catalysis" (D. D. Eley, P. W. Selwood, and P. B. Weisz, Eds.), Vol. 12, p. 31. Academic Press, New York, 1960.
6. Packer, K. J., *in* "Progress in NMR Spectroscopy" (J. M. Emsley, J. Feeney, and L. H. Sutcliffe, Eds.), Vol. 3, p. 81. Pergamon, London, 1968.

7. Pfeifer, H., *in* "NMR" (P. Diehl, E. Fluck, and R. Kosfeld, Eds.), Vol. 7, p. 53. Springer-Verlag, New York, 1972.
8. Resing, H. A., *Advan. Mol. Relaxation Processes* **1,** 109 (1967–68).
9. O'Reilly, D. E., Leftin, H. P., and Hall, W. K., *J. Chem. Phys.* **29,** 970 (1958).
10. Hall, W. K., Leftin, H. P., Cheselske, F. J., and O'Reilly, D. E., *J. Catal.* **2,** 506 (1963).
11. Pearson, R. M., *J. Catal.* **23,** 388 (1971).
12. Hall, W. K., private communication.
13. Schwarz, J. A., *J. Vac. Sci. Technol.* **12,** 321 (1975).
14. Kearby, K., PhD thesis, Univ. of Illinois, 1937.
15. Schwarz, J. A., private communication.
16. Vaughan, R. W., Elleman, D. D., Stacey, L. M., Rhim, W.-K., and Lee, J. W., *Rev. Sci. Instrum.* **43,** 1356 (1972).
17. Rhim, W.-K., Elleman, D. D., and Vaughan, R. W., *J J. Chem. Phys.* **59,** 3740 (1973).
18. Relcom, Mountain View, Calif.
19. Avantek, Inc., Santa Clara, Calif.
20. Abragam, A., "The Principles of Nuclear Magnetism," Oxford Univ. Press, London, 1961.
21. Vaughan, R. W., *in* "Annual Reviews in Materials Science" (R. A. Huggins, R. H. Bube, and R. W. Roberts, Eds.), Vol. 4, p. 21. Annu. Rev., Palo Alto, 1974, and references therein.
22. Farrar, T. C., and Becker, E. D., "Pulse and Fourier Transform NMR." Academic Press, New York, 1971.
23. Rhim, W.-K., Elleman, D. D., Schreiber, L. B., and Vaughan, R. W., *J. Chem. Phys.* **60,** 4595 (1974).
24. Dybowski, C. R., and Vaughan, R. W., *Macromolecules* **8,** 50 (1975).
25. Bloembergen, N., and Rowland, T. J., *Phys. Rev.* **97,** 1679 (1955).
26. Davydov, V. Y., Zhuravlev, L. T., and Kiselev, A. V., *Trans. Faraday Soc.* **60,** 2254 (1964).
27. Freude, D., Müller, D., and Schmiedel, H., *Surface Sci.* **25,** 289 (1971).
28. Rakvin, B., and Herak, J. N., *J. Magn. Resonance* **13,** 94 (1974), and references therein.
29. Peri, J. B., and Hensley, Jr., A. L., *J. Phys. Chem.* **72,** 2926 (1968).
30. Osborn, J. A., *Phys. Rev.* **67,** 351 (1945).
31. Haeberlen, U., *Proc. Specialized Colloque Ampère, 1st* (Krakow, Poland) p. 28 (1973); Vaughan, R. W., Rhim, W.-K., and Elleman, D. D., *Proc. Specialized Colloque Ampère, 1st* (Krakow, Poland) p. 129 (1973); Haubenreisser, U., and Schnabel, B., *Proc. Specialized Colloque Ampère, 1st* (Krakow, Poland) p. 140 (1973); Van Hecke, P., Weaver, J. C., Neff, B. L., and Waugh, J. S., *Proc. Specialized Colloque Ampère, 1st* (Krakow, Poland) p. 143 (1973); *J. Chem. Phys.* **60,** 1668 (1974); Haeberlen, U., and Kohlschütter, U., *Chem. Phys.* **2,** 76 (1973); Raber, H., Brunger, G., and Mehring, M., *Chem. Phys. Lett.* **23,** 400 (1973); Haeberlen, U., Kohlschütter, U., Kempt, J., Spiess, H. W., and Zimmermann, H., *Chem. Phys.* **3,** 248 (1974); Willsch, R., Burghoff, U., Müller, R., Rosenberger, H., Scheler, G., Pettig, M., and Schnabel, B., *Proc. Ampère Congr. 18th* (Nottingham) p. 553, 1974.
32. Schreiber, L. B., and Vaughan, R. W., *Chem. Phys. Lett.* **28,** 586 (1974).
33. Young, G. J., *J. Colloid Sci.* **13,** 67 (1958).
34. Hockey, J. A., and Pethica, B. A., *Trans. Faraday Soc.* **57,** 2247 (1961).
35. Haldeman, R. G., and Emmett, P. H., *J. Amer. Chem. Soc.* **78,** 2917 (1956).
36. Basila, M. R., *J. Phys. Chem.* **66,** 2223 (1962).